

Encapsulated Guest–Host Dynamics: Guest Rotational Barriers and Tumbling as a Probe of Host Interior Cavity Space

Jeffrey S. Mugridge, Géza Szigethy, Robert G. Bergman,* and Kenneth N. Raymond*

Department of Chemistry, University of California, Berkeley, and Chemical Science Division, Lawrence Berkeley National Laboratory, Berkeley, California 94720-1460, United States

Received August 24, 2010; E-mail: rbergman@berkeley.edu; raymond@socrates.berkeley.edu

Abstract: The supramolecular host assembly $[\text{Ga}_4\text{L}_6]^{12-}$ (**1**; L = 1,5-bis[2,3-dihydroxybenzamido]naphthalene) encapsulates cationic guest molecules within its hydrophobic cavity and catalyzes a variety of chemical transformations within its confined interior space. Despite the well-defined structure, the host ligand framework and interior cavity are very flexible and **1** can accommodate a wide range of guest shapes and sizes. These observations raise questions about the steric effects of confinement within **1** and how encapsulation fundamentally changes the motions of guest molecules. Here we examine the motional dynamics (guest bond rotation and tumbling) of encapsulated guest molecules to probe the steric consequences of encapsulation within host **1**. Encapsulation is found to increase the Ph–CH₂ bond rotational barrier for *ortho*-substituted benzyl phosphonium guest molecules by 3 to 6 kcal/mol, and the barrier is found to depend on both guest size and shape. The tumbling dynamics of guests encapsulated in **1** were also investigated, and here it was found that longer, more prolate-shaped guest molecules tumble more slowly in the host cavity than larger but more spherical guest molecules. The prolate guests reduce the host symmetry from *T* to *C*₁ in solution at low temperatures, and the distortion of the host framework that is in part responsible for this symmetry reduction is observed directly in the solid state. Analysis of guest motional dynamics is a powerful method for interrogating host structure and fundamental host–guest interactions.

Introduction

The active sites of enzymes can dramatically affect the physical properties and reactivity of bound substrate molecules. Hydrophobic protein binding pockets present substrates with an environment that is sterically and electronically different from that in aqueous solution, and this forms the basis for the remarkable selectivity and rate accelerations observed in many biological systems.^{1,2} Synthetic supramolecular host–guest systems can function in much the same way. Encapsulated guest molecules interact with a host cavity through noncovalent interactions and typically experience a very different steric and electronic environment inside the host than in bulk solution. The unique interior environment of supramolecular host molecules has been shown to stabilize reactive species,^{3–7} promote

formation of unusual or labile guest conformations,^{8–10} alter guest reactivity,^{11–16} and catalyze a variety of chemical transformations.^{17–21}

Insight into the remarkable behaviors described above comes from a detailed understanding of the fundamental host–guest interactions involved in these supramolecular systems. One approach to this is the analysis of encapsulated guest conformational and rotational dynamics, which can give information

- (1) Warshel, A.; Sharma, P. K.; Kato, M.; Xiang, Y.; Liu, H.; Olsson, M. H. M. *Chem. Rev.* **2006**, *106*, 3210–3235.
- (2) Estell, D. A.; Graycar, T. P.; Miller, J. V.; Powers, D. B.; Wells, J. A.; Burnier, J. P.; Ng, P. G. *Science* **1986**, *233*, 659–663.
- (3) Cram, D. J.; Tanner, M. E.; Thomas, R. *Angew. Chem., Int. Ed. Engl.* **1991**, *30*, 1024–1027.
- (4) Warmuth, R.; Marvel, M. A. *Angew. Chem., Int. Ed.* **2000**, *39*, 1117–1119.
- (5) Iwasawa, T.; Hooley, R. J.; Rebek, J., Jr. *Science* **2007**, *317*, 493–496.
- (6) Mal, P.; Breiner, B.; Rissanen, K.; Nitschke, J. R. *Science* **2009**, *324*, 1697–1699.
- (7) Fiedler, D.; Bergman, R. G.; Raymond, K. N. *Angew. Chem., Int. Ed.* **2006**, *45*, 745–748.

- (8) Tashiro, S.; Kobayashi, M.; Fujita, M. *J. Am. Chem. Soc.* **2006**, *128*, 9280–9281.
- (9) Kusakawa, T.; Fujita, M. *J. Am. Chem. Soc.* **1999**, *121*, 1397–1398.
- (10) Scarso, A.; Trembleau, L.; Rebek, J., Jr. *J. Am. Chem. Soc.* **2004**, *126*, 13512–13518.
- (11) Nishioka, Y.; Yamaguchi, T.; Yoshizawa, M.; Fujita, M. *J. Am. Chem. Soc.* **2007**, *129*, 7000–7001.
- (12) Leung, D. H.; Bergman, R. G.; Raymond, K. N. *J. Am. Chem. Soc.* **2006**, *128*, 9781–9797.
- (13) Hou, J.; Ajami, D.; Rebek, J., Jr. *J. Am. Chem. Soc.* **2008**, *130*, 7810–7811.
- (14) Kuil, M.; Soltner, T.; van Leeuwen, P. W. N. M.; Reek, J. N. H. *J. Am. Chem. Soc.* **2006**, *128*, 11344–11345.
- (15) Oshovsky, G. V.; Reinhoudt, D.; Verboom, W. *Angew. Chem., Int. Ed.* **2007**, *46*, 2366–2393.
- (16) Purse, B. W.; Gissot, A.; Rebek, J., Jr. *J. Am. Chem. Soc.* **2005**, *127*, 11222–11223.
- (17) Pluth, M. D.; Bergman, R. G.; Raymond, K. N. *Acc. Chem. Res.* **2009**, *42*, 1650–1659.
- (18) van Leeuwen, P. W. N. M. *Supramolecular catalysis*; Wiley-VCH: 2008.
- (19) Yoshizawa, M.; Klosterman, J.; Fujita, M. *Angew. Chem., Int. Ed.* **2009**, *48*, 3418–3438.
- (20) Richeter, S.; Rebek, J., Jr. *J. Am. Chem. Soc.* **2004**, *126*, 16280–16281.
- (21) Zelder, F. H.; Rebek, J., Jr. *J. Am. Chem. Commun.* **2006**, *75*, 753–754.

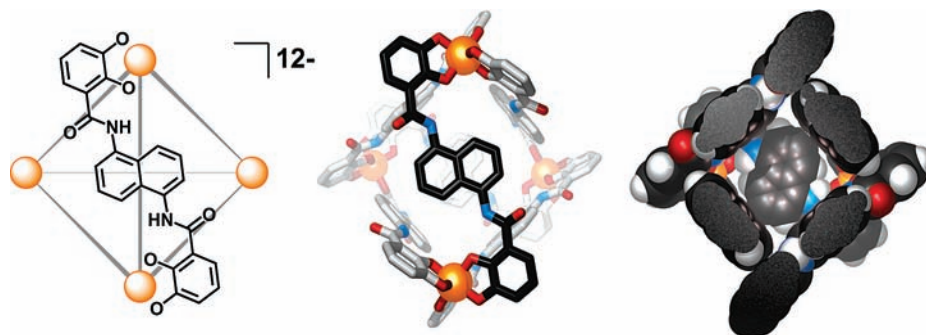


Figure 1. Supramolecular assembly **1** as viewed down the C_2 axis of the tetrahedron. (Left) Schematic of **1** with only one ligand shown for clarity; (center) ball and stick model with one ligand highlighted; (right) space-filling model with the front half of the assembly cut away so that the interior cavity is visible.

about the effects of guest confinement within a host cavity. Many researchers have investigated how guest encapsulation or complexation perturbs the motional dynamics of both host and guest molecules.^{22–32} In particular, Rebek and co-workers have extensively examined the physical organic chemistry of molecules confined within their hydrogen-bonded molecular capsules (what they have called “inner space”).^{33–37} Generally, these studies demonstrate how confinement within a host cavity restricts the conformational, rotational, and/or translational space available to guest molecules. Such restriction of guest motional space can promote an increased local concentration of reactants or stabilization of reactive guest conformations, leading to a unique reactivity or catalysis.

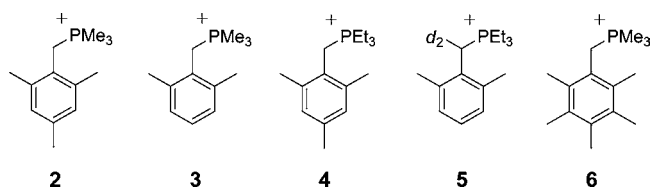
Over the past decade, this effort has investigated the host–guest dynamics and reactivity of the self-assembled $[Ga_4L_6]^{12-}$ supramolecular host (**1**; Figure 1; $L = 1,5$ -bis[2,3-dihydroxybenzamido]naphthalene). The T -symmetric assembly **1** is composed of four Ga(III) metal centers located at the vertices of a tetrahedron, whose edges are spanned by six naphthalene-based catecholamide ligands.^{38,39} The supramolecular complex contains a hydrophobic interior cavity which

can act as a host for suitably sized monocationic^{40–42} and neutral^{43,44} guest molecules. The host structure is very flexible: guest molecules can enter and exit host **1** by squeezing through expandable apertures in the ligand framework, and the interior cavity can distort to accommodate different guest shapes and sizes.^{45,46} Host interior cavity volumes ranging from 250 to 450 Å³ have been observed in the solid state.⁴⁷ The confinement experienced by guests encapsulated within the host cavity has been exploited to catalyze pericyclic rearrangements by binding guests in a reactive conformation,^{48–50} impose enantioselectivity on these rearrangements,⁵¹ and alter substrate selectivity in C–H bond activation reactions with an encapsulated iridium complex.⁵²

While the above examples of encapsulated reactivity suggest that guests are sterically constrained within the host cavity, the significance and extent of these confinement effects remain unclear given the dramatic flexibility of the host framework. Furthermore, it was recently observed in one system that amide bond rotation is **accelerated** inside of host **1** compared to its rate in bulk solution.⁵³ The electronic stabilization of the hydrophobic transition state for amide bond rotation apparently overcomes any steric effects which might serve to hinder that rotation. Herein, we use the motional dynamics of *ortho*-substituted benzyl trialkyl phosphonium guest molecules to quantitatively probe the steric consequences of guest encapsula-

- (22) Brouwer, E. B.; Enright, G. D.; Ratcliffe, C. I.; Facey, G. A.; Ripmeester, J. A. *J. Phys. Chem. B* **1999**, *103*, 10604–10616.
- (23) Chapman, R. G.; Sherman, J. C. *J. Org. Chem.* **2000**, *65*, 513–516.
- (24) Frischmann, P. D.; Facey, G. A.; Ghi, P. Y.; Gallant, A. J.; Bryce, D. L.; Lejl, F.; MacLachlan, M. J. *J. Am. Chem. Soc.* **2010**, *132*, 3893–3908.
- (25) Kitagawa, H.; Kobori, Y.; Yamanaka, M.; Yoza, K.; Kobayashi, K. *Proc. Natl. Acad. Sci. U.S.A.* **2009**, *106*, 10444–10448.
- (26) Kulasekharan, R.; Jayaraj, N.; Porel, M.; Choudhury, R.; Sundaresan, A. K.; Parthasarathy, A.; Ottaviani, M. F.; Jockusch, S.; Turro, N. J.; Ramamurthy, V. *Langmuir* **2010**, *26*, 6943–6953.
- (27) Kurdistani, S. K.; Robbins, T. A.; Cram, D. J. *J. Chem. Soc., Chem. Commun.* **1995**, 1259–1260.
- (28) Kusakawa, T.; Yoshizawa, M.; Fujita, M. *Angew. Chem., Int. Ed.* **2001**, *40*, 1879–1884.
- (29) Mileo, E.; Yi, S.; Bhattacharya, P.; Kaifer, A. *Angew. Chem., Int. Ed.* **2009**, *48*, 5337–5340.
- (30) Nishimura, N.; Yoza, K.; Kobayashi, K. *J. Am. Chem. Soc.* **2010**, *132*, 777–790.
- (31) Tominaga, M.; Tashiro, S.; Aoyagi, M.; Fujita, M. *Chem. Commun.* **2002**, 2038–2039.
- (32) Vysotsky, M. O.; Pop, A.; Broda, F.; Thondorf, I.; Böhmer, V. *Chem.—Eur. J.* **2001**, *7*, 4403–4410.
- (33) Ajami, D.; Rebek, J., Jr. *J. Org. Chem.* **2009**, *74*, 6584–6591.
- (34) Hooley, R. J.; Shenoy, S. R.; Rebek, J., Jr. *Org. Lett.* **2008**, *10*, 5397–5400.
- (35) O’Leary, B. M.; Grotzfeld, R. M.; Rebek, J., Jr. *J. Am. Chem. Soc.* **1997**, *119*, 11701–11702.
- (36) Purse, B. W.; Butterfield, S. M.; Ballester, P.; Shivanyuk, A.; Rebek, J., Jr. *J. Org. Chem.* **2008**, *73*, 6480–6488.
- (37) Rebek, J., Jr. *Acc. Chem. Res.* **2009**, *42*, 1660–1668.
- (38) Caulder, D. L.; Powers, R. E.; Parac, T. N.; Raymond, K. N. *Angew. Chem., Int. Ed.* **1998**, *37*, 1840–1843.
- (39) Caulder, D. L.; Raymond, K. N. *Acc. Chem. Res.* **1999**, *32*, 975–982.

- (40) Parac, T. N.; Caulder, D. L.; Raymond, K. N. *J. Am. Chem. Soc.* **1998**, *120*, 8003–8004.
- (41) Parac, T. N.; Scherer, M.; Raymond, K. N. *Angew. Chem., Int. Ed.* **2000**, *39*, 1239–1242.
- (42) Fiedler, D.; Pagliero, D.; Brumaghim, J. L.; Bergman, R. G.; Raymond, K. N. *Inorg. Chem.* **2004**, *43*, 846–848.
- (43) Biros, S. M.; Bergman, R. G.; Raymond, K. N. *J. Am. Chem. Soc.* **2007**, *129*, 12094–12095.
- (44) Hastings, C. J.; Pluth, M. D.; Biros, S. M.; Bergman, R. G.; Raymond, K. N. *Tetrahedron* **2008**, *64*, 8362–8367.
- (45) Davis, A. V.; Raymond, K. N. *J. Am. Chem. Soc.* **2005**, *127*, 7912–7919.
- (46) Davis, A. V.; Fiedler, D.; Seeber, G.; Zahl, A.; van Eldik, R.; Raymond, K. N. *J. Am. Chem. Soc.* **2006**, *128*, 1324–1333.
- (47) Pluth, M. D.; Johnson, D. W.; Szigethy, G.; Davis, A. V.; Teat, S. J.; Oliver, A. G.; Bergman, R. G.; Raymond, K. N. *Inorg. Chem.* **2009**, *48*, 111–120.
- (48) Fiedler, D.; van Halbeek, H.; Bergman, R. G.; Raymond, K. N. *J. Am. Chem. Soc.* **2006**, *128*, 10240–10252.
- (49) Fiedler, D.; Leung, D. H.; Bergman, R. G.; Raymond, K. N. *Acc. Chem. Res.* **2005**, *38*, 349–358.
- (50) Hastings, C. J.; Fiedler, D.; Bergman, R. G.; Raymond, K. N. *J. Am. Chem. Soc.* **2008**, *130*, 10977–10983.
- (51) Brown, C. J.; Bergman, R. G.; Raymond, K. N. *J. Am. Chem. Soc.* **2009**, *131*, 17530–17531.
- (52) Leung, D. H.; Fiedler, D.; Bergman, R. G.; Raymond, K. N. *Angew. Chem., Int. Ed.* **2004**, *43*, 963–966.
- (53) Pluth, M. D.; Bergman, R. G.; Raymond, K. N. *J. Org. Chem.* **2008**, *73*, 7132–7136.

Chart 1. *Ortho*-Substituted Benzyl Phosphonium Guests⁵⁴

tion within **1**. Encapsulation is found to raise guest bond rotational barriers by 3–6 kcal/mol and prolate-shaped guest molecules are found to tumble more slowly inside the host cavity compared with the tumbling of larger, but more spherically shaped, guest molecules.

Results and Discussion

Encapsulated Guest Rotational Barriers. A series of *ortho*-substituted benzyl trialkyl phosphonium cations (**2–6**, Chart 1) were prepared as guest molecules to probe the effects of confinement within **1** on the motional dynamics of encapsulated guests. Since host **1** has purely rotational T symmetry (i.e., there is no mirror symmetry in the host cavity), the aromatic *ortho* methyl groups (as well as the aromatic *meta* substituents) for encapsulated guests **2–6** are related only by rotation about the Ph–CH₂ bond. Therefore, the *ortho* (or *meta*) substituents will be chemically inequivalent if Ph–CH₂ bond rotation is slow on the NMR time scale. Guests **2–6** are cleanly encapsulated in **1** in CD₃OD solution, and two signals corresponding to the *ortho* methyl groups of the encapsulated guest are observed by ¹H NMR for each host–guest complex at room temperature (Figure 2).

Selective inversion recovery (SIR) NMR experiments⁵⁵ were used to measure the rate of Ph–CH₂ bond rotation for encapsulated guests **2–5**. One of the chemically inequivalent *ortho* or *meta* substituents was selectively spin-labeled (its ¹H NMR resonance was inverted), and a variable mixing time was waited before collecting a 1D ¹H NMR spectrum. The rate of exchange between the inverted resonance and its decoalesced partner (the other *ortho* or *meta* guest substituent) can be derived by monitoring the change in both integrals as a function of the variable mixing time (Figure 3, Figure 4 left). Since Ph–CH₂ bond rotation of the encapsulated guest relates the inequivalent *ortho* or *meta* substituents, this SIR experiment directly measures the rate of Ph–CH₂ bond rotation.

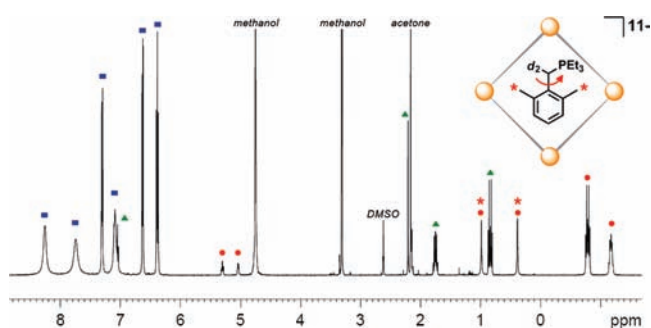


Figure 2. ¹H NMR spectrum of [**5 C 1**]¹¹⁻ in CD₃OD at 296 K (where C denotes encapsulation), with schematic of encapsulated guest Ph–CH₂ bond rotation. The total host and guest concentrations are [**1**] = 7 mM and [**5**] = 14 mM. Since Ph–CH₂ bond rotation is slow on the NMR time scale, *ortho* methyl groups (*) are chemically inequivalent and therefore exhibit different ¹H NMR chemical shifts. Encapsulated guest (●), exterior guest (▲), and host (■) resonances are also labeled.

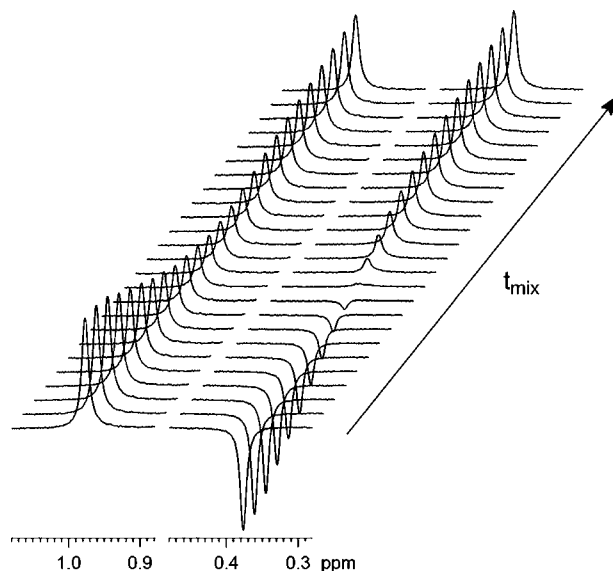


Figure 3. ¹H NMR spectra at different mixing times (t_{mix}) from the SIR experiment with [**5 C 1**]¹¹⁻ in CD₃OD at 296 K. As the inverted ¹H NMR resonance (right) corresponding to one of the *ortho* aromatic methyl groups of guest **5** exchanges via Ph–CH₂ bond rotation, the intensity of its uninverted partner (left) initially decreases due to this exchange process. At longer mixing times, the intensity of both signals increases due to T_1 relaxation.

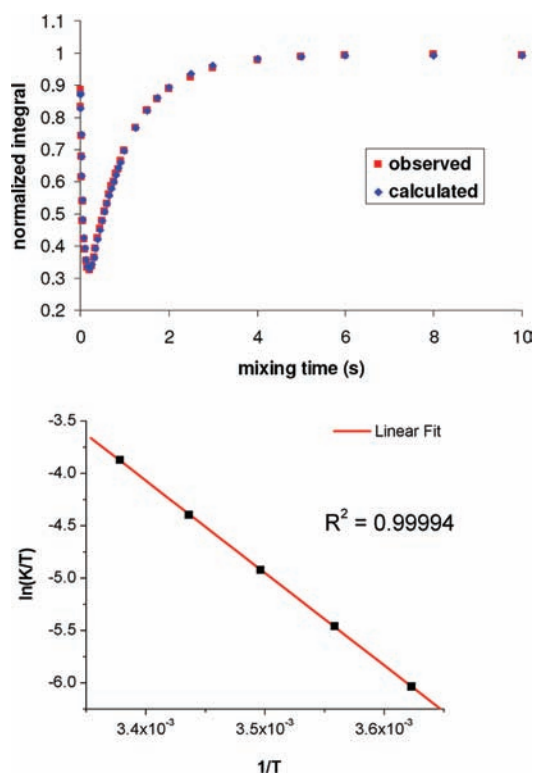
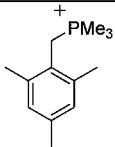
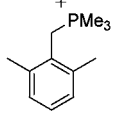
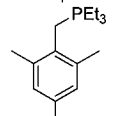
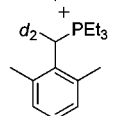


Figure 4. (Top) Observed and calculated integrals from an SIR experiment with [**5 C 1**]¹¹⁻ in CD₃OD at 296 K for one of the exchanging Ar–CH₃ resonances. (Bottom) Eyring plot used to determine the activation parameters for Ph–CH₂ bond rotation of [**5 C 1**]¹¹⁻ in CD₃OD.

It should be noted here that another possible mechanism for exchange between *ortho* or *meta* guest substituents is guest ejection, rapid Ph–CH₂ bond rotation in solution, and re-encapsulation. If guest exchange occurs on a comparable time scale to Ph–CH₂ bond rotation, then the apparent rate of bond rotation would be affected by guest molecules exiting and

Table 1. Activation Parameters for Ph–CH₂ Bond Rotation of Phosphonium Guest Molecules Encapsulated within Host **1** in CD₃OD^a

guest	$\Delta G^\ddagger(\text{rotation}), 298 \text{ K}$ (kcal/mol)	$\Delta H^\ddagger(\text{rotation})$ (kcal/mol)	$\Delta S^\ddagger(\text{rotation})$ (cal/mol K)	guest volume ^a (Å ³)	
	2	19.1(5)	22.1(6)	10.0(3)	208
	3	17.1(1)	19.4(1)	7.80(5)	196
	4	17.3(4)	20.6(5)	11.1(3)	260
	5	16.3(1)	17.53(8)	4.35(2)	247

^a Solvent accessible volumes were calculated in UCSF Chimera.⁵⁶

entering the host. This is not the case for guests **2–5**; guest exchange was found to be at least 1 order of magnitude slower than Ph–CH₂ bond rotation for each of these guest molecules (see Supporting Information). Furthermore, for guest **2**, whose guest exchange rate and Ph–CH₂ bond rotation rate were closest in magnitude, it was found that the Ph–CH₂ rotation rate was invariant with the concentration of **2** or the concentration of the [2 C 1]¹¹⁻ host–guest complex. Therefore, although interior–exterior guest exchange does occur in these systems, it is significantly slower than Ph–CH₂ bond rotation and negligibly affects measurement of the latter.

The rates of encapsulated Ph–CH₂ bond rotation for guests **2–5** were measured at different temperatures, and Eyring analysis was used to determine activation parameters for the rotational motion (Figure 4, Table 1). The observed Ph–CH₂ bond rotational barriers for the encapsulated guests range from 16 to 19 kcal/mol, and the rotational barrier is dominated by enthalpy. One might have expected larger guest molecules to be more sterically confined within the host cavity and thus have the largest Ph–CH₂ rotational barriers, but this trend is not observed. In fact, when comparing the guests **2** versus **4** and **3** versus **5**, we find that increasing the steric bulk by adding PEt₃ groups instead of PMe₃ groups actually lowers the rotational barrier. This may be a result of the bulkier PEt₃ group creating a larger and more spherical host cavity, such that the energetic penalty for that expansion is paid upon encapsulation, and the enlarged interior cavity allows for more facile bond rotation. On the other hand, comparing guests **2** versus **3** and **4** versus **5**, we find that addition of the *para* methyl group to the aromatic ring increases the bond rotational barrier. Here, it may be the case that addition of the *para* methyl group forces the guests'

ortho methyl groups further from the center of the interior cavity and closer to the host walls, impeding the rotational process. These explanations are necessarily somewhat speculative, but the observed Ph–CH₂ bond rotational barriers for encapsulated guests unambiguously demonstrate that the motional dynamics of the encapsulated guests are both size and shape dependent.

Rotational Barriers in Bulk Solution. In order to determine how confinement within the host cavity affects guest motional dynamics, we wanted to compare the encapsulated bond rotational barriers reported above with those measured in bulk solution. Unfortunately, the Ph–CH₂ bond rotational barriers of guests **2–5** cannot be measured in bulk solution because mirror symmetry relates the *ortho* and *meta* aromatic substituents, meaning these substituents will be chemically equivalent regardless of the bond rotational rate. However, asymmetric substitution of the aromatic ring at only one *meta* position breaks that mirror symmetry, making the now enantiotopic benzyl CH₂ protons chemically inequivalent as Ph–CH₂ bond rotation becomes slow on the NMR time scale (Figure 5). Activation parameters for Ph–CH₂ bond rotation of benzyl phosphonium cations **7** and **8** in CD₃OD were measured using SIR experiments on the decoalesced benzyl protons (Table 2).

The Ph–CH₂ bond rotational barrier for phosphonium cations **7** and **8** is approximately 13 kcal/mol in CD₃OD. Assuming that the *meta* and *para* substituents negligibly affect this rotational barrier, guests **2–5** must also have rotational barriers close to 13 kcal/mol in bulk CD₃OD solution. Thus, encapsulation within host **1** raises the Ph–CH₂ bond rotational barrier by 3–6 kcal/mol for guests **2–5**. This corresponds to between a 100- and 15 000-fold decrease in the rate of internal bond rotation upon encapsulation of guests **2–5**. To confirm that this dramatic change in the guest motional dynamics was due to steric confinement within the host, rather than an electronic effect imparted by the nonpolar, hydrophobic interior cavity space, the Ph–CH₂ rotational barrier for cation **7** was measured in a nonpolar solvent. In toluene-*d*₈ (with 10% by volume CD₃OD to aid solubility), the Ph–CH₂ rotational barrier for cation **7** was found to be within error of that measured in

(55) Bain, A. D.; Cramer, J. A. *J. Magn. Reson. A* **1996**, *118*, 21–27.

(54) Guest **5** was deuterated at the benzyl position to alleviate peak overlap problems in the encapsulated guest region of the ¹H NMR spectrum. Peak overlap was not an issue with the other guest molecules studied.

(56) Pettersen, E. F.; Goddard, T. D.; Huang, C. C.; Couch, G. S.; Greenblatt, D. M.; Meng, E. C.; Ferrin, T. E. *J. Comput. Chem.* **2004**, *25*, 1605–1612.

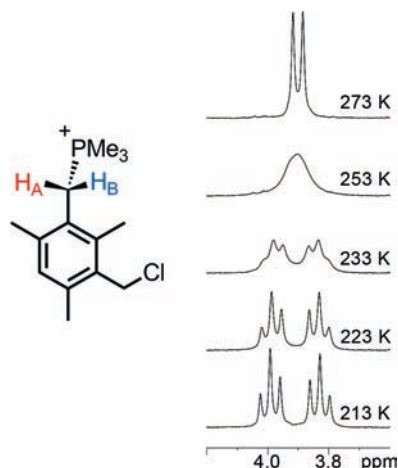


Figure 5. (Left) Benzyl phosphonium cation **7**. Enantiotopic benzyl protons H_A and H_B become chemically inequivalent as Ph-CH₂ bond rotation becomes slow on the NMR time scale due to the asymmetric ring substitution. (Right) Variable temperature ¹H NMR spectra showing decoalescence of H_A and H_B for cation **7** in CD₃OD.

CD₃OD (see Supporting Information). This suggests that the rotational barrier is insensitive to changes in the cation's electronic environment and that, despite the flexibility of the host framework and interior cavity, steric confinement within **1** is responsible for the significant increase in guest Ph-CH₂ bond rotational barriers observed upon encapsulation.

Guest Tumbling Dynamics. The tumbling motion of encapsulated guest molecules also provides some information about the effects of confinement within **1** and how guest size and shape affect these motional dynamics. When the host-guest complexes [2 ⊂ 1]¹¹⁻ – [6 ⊂ 1]¹¹⁻ are cooled, a reduction in host symmetry is observed as the tumbling, or reorientation of the encapsulated guest within the host cavity, becomes slow on the NMR time scale (Figure 6). The more prolate guests **2** and **4** readily reduce the symmetry of host **1** to C₁ at 285 and 273 K, respectively. The assignment of C₁ symmetry for these host-guest complexes is based on the observation of a very large number of host aromatic C-H resonances and 11 of the 12 distinct amide N-H resonances expected for C₁ symmetry (significantly more than the 6 or 4 N-H resonances expected for C₂ or C₃ host symmetry, respectively) at low temperatures. Additionally, further cooling of complex [4 ⊂ 1]¹¹⁻ to 253 K reveals all 12 amide NH resonances and 2D ¹³C-¹H NMR experiments further confirm the assignment of C₁ host symmetry (see Supporting Information for spectra).

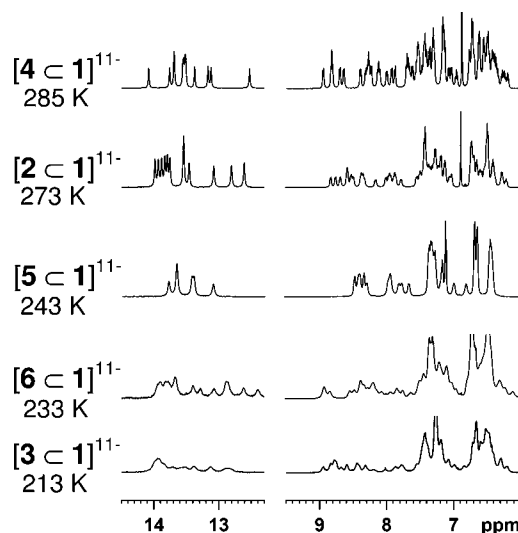
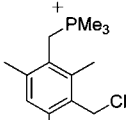
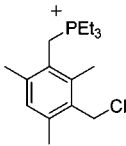


Figure 6. ¹H NMR spectra collected at 600 MHz of host-guest complexes with guests **2**–**6** in CD₃OH at the low temperatures required to observe a reduction in host symmetry for each complex. For clarity, only the host amide N-H region (14–12 ppm) and host aromatic C-H region (9–6 ppm) are shown in each spectrum. The spectra are ordered by the temperature required for host symmetry reduction, such that the host-guest complexes shown at the top break the symmetry at higher temperatures, while those at the bottom of the figure require lower temperatures.

The guest molecules **3**, **5**, and **6** require lower temperatures to break the host symmetry. The symmetry of these host-guest complexes is ambiguous due to broad and/or overlapping aromatic C-H and amide N-H host resonances, but it is clear that the *T* symmetry of **1** is broken at these temperatures. Unfortunately, these broad and overlapping host resonances and the complexity of decoalescence from *T* to C₁ or other symmetries preclude quantitative measurement of the barrier to guest tumbling inside of **1**. However, based on the temperatures required to break the host symmetry, we can make the qualitative observation that the more prolate guests **2** and **4** tumble more slowly inside of host **1** than the more spherical guests **3**, **5**, and **6**. Furthermore, comparing guests **2** versus **6**, we see that the larger guest **6**, which has additional methyl groups at the *meta* positions, actually tumbles more easily within the host, presumably due to the larger and more spherical cavity required to encapsulate guest **6**.

To provide further support for this argument, molecular-mechanics-based conformational searching (MacroModel,⁵⁷ OPLS 2005⁵⁸) was carried out on models of the host-guest complexes [2 ⊂ 1]¹¹⁻ and [6 ⊂ 1]¹¹⁻. The void-space cavities

Table 2. Activation Parameters for Ph-CH₂ Bond Rotation of Asymmetric Phosphonium Cations in Bulk CD₃OD

cation	$\Delta G^\ddagger(\text{rotation}), 298 \text{ K}$ (kcal/mol)	$\Delta H^\ddagger(\text{rotation})$ (kcal/mol)	$\Delta S^\ddagger(\text{rotation})$ (cal/mol K)
 7	13.4(6)	7.9(3)	-18.5(9)
 8	13(1)	8.8(9)	-12(2)

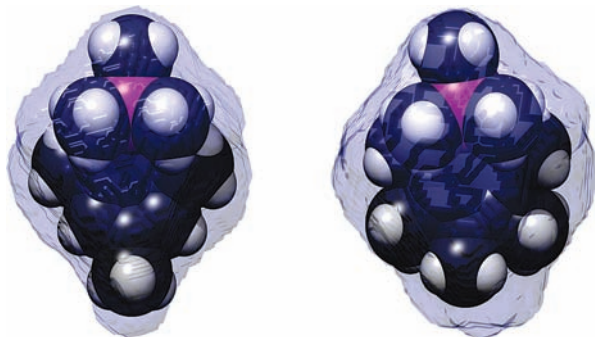


Figure 7. Space-filling models of guests **2** (left) and **6** (right), each surrounded by the calculated void space inside of **1** for the modeled host–guest complexes. Guest **6** creates a larger and rounder host cavity space.

for the lowest energy host–guest conformations were then calculated using Voidoo.^{59,60} The calculated host interior cavity for guest **6** (502 Å³) is larger and more spherical than the cavity calculated for guest **2** (440 Å³). Figure 7 shows the space-filling models and calculated void space cavities for guests **2** and **6**. The effect of the additional methyl groups on guest **6** is to expand the host cavity to a larger volume and more spherical shape, which facilitates the tumbling of guest **6** within **1**, relative to the more prolate guest **2**.

Solid-State Structure of [2 ⊂ 1]¹¹⁻. Single crystals suitable for X-ray diffraction studies were obtained for the host–guest complex [2 ⊂ 1]¹¹⁻. The solid-state structure of this complex provides some insight into the origins of the host symmetry reduction observed in solution. Encapsulated guest **2** sits within the host cavity such that its *para* methyl group points directly toward, and extends partially into, one of the apertures in the host framework (Figure 8). The result is that this particular aperture is significantly dilated, while the three other apertures in the host framework are contracted (Figure 9). The desymmetrization of host **1** observed in the solid state is consistent with the modeling studies presented above and demonstrates how the 2-fold rotational symmetry of the host is destroyed by the length of guest **2**, which forces a distortion of the host framework. Rotation of the guest about the host 3-fold axis could maintain C₃ symmetry for the host–guest complex in solution, but as this process becomes slow at lower temperatures, the complex is reduced to C₁ symmetry.

Unrelated to the above discussion of guest motional dynamics, the expansion of one of the apertures in the host framework is significant for host–guest exchange dynamics. We have long proposed that guest molecules enter and exit the host cavity by squeezing through the apertures in the host framework. Kinetic experiments,⁴⁶ isotope effects,⁶¹ the formation of dangling arm complexes,⁶² and modeling studies⁴⁵ all demonstrate that this is the mechanism for guest exchange, but there has not been direct structural evidence for host aperture distortion. The

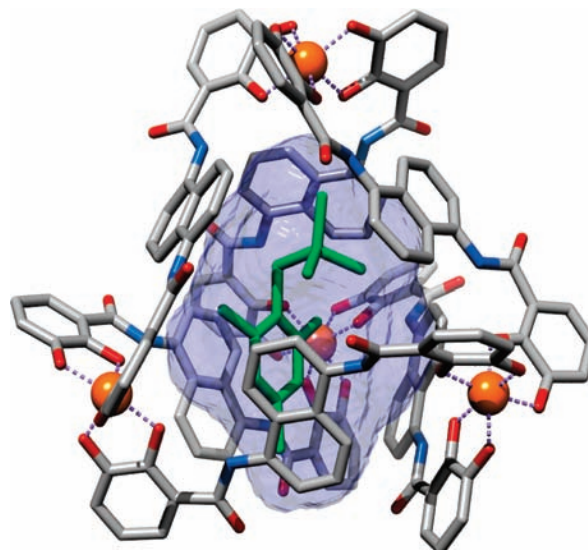


Figure 8. Solid-state structure of [2 ⊂ 1]¹¹⁻ with exterior phosphonium and potassium cations, interior guest disorder, and solvent omitted for clarity. The encapsulated guest **2** is shown in green, and the calculated void space (367 Å³) is shown in blue. The void space is seen to extend well into one of the host apertures, which is distorted by the *para* methyl group of encapsulated **2**.

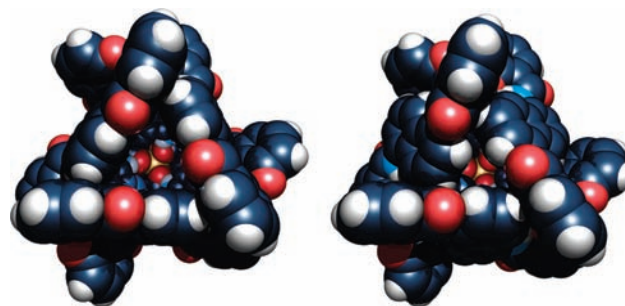


Figure 9. Space-filling representation of the host framework from the solid-state structure of [2 ⊂ 1]¹¹⁻ as viewed down the dilated aperture (left) and one of three other contracted apertures (right).

aperture dilation observed in the solid-state structure of [2 ⊂ 1]¹¹⁻ is quite large: the area defined by the H–H distances among the different naphthalene rings that compose the C₃-symmetric apertures is more than twice as large for the dilated aperture than for the other contracted apertures. Although this distortion is not nearly large enough to allow the passage of typical alkyl or benzyl ammonium/phosphonium guest molecules, it provides direct structural evidence supporting an aperture-based guest exchange mechanism.

Conclusion

To explore the steric environment experienced by guest molecules confined within supramolecular host **1**, the rotational and tumbling dynamics for a series of encapsulated benzyltri-alkyl phosphonium cations were investigated. The motional dynamics of the encapsulated guest molecules are found to depend strongly on both guest size and shape. While one might expect that the motions of larger guest molecules confined within the cavity of **1** would be more restricted, this was often not true. In many cases, an increase in guest size was observed to facilitate both guest rotational and tumbling motions, which we interpret as the result of a corresponding increase in overall cavity size or more spherical cavity shape. The bond rotational

(57) MacroModel; Schrodinger: New York, NY, 2010.

(58) Jorgensen, W. L.; Tirado-Rives, J. *Proc. Natl. Acad. Sci. U.S.A.* **2005**, *102*, 6665–6670.

(59) Kleywegt, G. J.; Jones, T. A. *Acta Crystallogr.* **1994**, *D50*, 178–185.

(60) Kleywegt, G. J.; Zou, J. Y.; Kjeldgaard, M.; Jones, T. A. *International Tables for Crystallography*; International Union of Crystallography, Kluwer Academic: Dordrecht, The Netherlands, 2001; Vol. F, Chapter 17.1, pp 353–356, 366–367.

(61) Mugridge, J. S.; Bergman, R.; Raymond, K. *Angew. Chem., Int. Ed.* **2010**, *49*, 3635–3637.

(62) Tiedemann, B. E. F.; Raymond, K. N. *Angew. Chem., Int. Ed.* **2006**, *45*, 83–86.

barriers for similar phosphonium cations measured in bulk solution indicate that encapsulation within host **1** raises the Ph–CH₂ bond rotational barrier by 3–6 kcal/mol. This large change in the rotational dynamics for encapsulated guest molecules demonstrates that, despite the flexibility of the host framework and the wide range of accessible cavity volumes, guest molecules experience a significantly confined steric environment within the host cavity.

In summary, we have shown that the motional dynamics of encapsulated guests can provide a sensitive probe of the host interior space. Furthermore, these dynamics can in principle provide fundamental information about how the host structure and flexibility change in different solvents or with different exterior counterions. These features of guest encapsulation are important for understanding the changes in guest behavior that underlie both stabilization of reactive species and host-mediated catalysis.

Experimental Section

General. Unless otherwise noted, manipulations were carried out using standard Schlenk and high-vacuum techniques and all chemicals were obtained from commercial suppliers and used without further purification. All glassware was oven-dried at 150 °C. All solvents were sparged with nitrogen prior to use. Diethyl ether was dried by passing the solvent through columns of activated alumina under nitrogen pressure.⁶³ Supramolecular host assembly K₁₁[**1**] was prepared as previously described³⁸ and stored under nitrogen. All host–guest complexes were prepared *in situ* by mixing 1 equiv of host K₁₁[**1**] with 2 equiv of guest in CD₃OD (~5% DMSO-*d*₆ was added to aid solubility) under a nitrogen atmosphere; the host–guest complexes were all formed quantitatively. 2 equiv of guest were used so that SIR experiments to measure the guest exchange kinetics (which require an exterior guest population) could be carried out on the same solution used to measure bond rotation. A host concentration of 7 mM was used for all rotational barrier and guest tumbling measurements. All SIR NMR experiments were carried out on a Bruker AV-500 NMR spectrometer, and all variable temperature ¹H NMR spectra used in the guest tumbling analysis were collected on a Bruker AV-600 NMR spectrometer. Chemical shifts are reported in parts per million (δ) relative to residual protic solvent resonances. For ³¹P{¹H} NMR spectra, chemical shifts are reported relative to a triethyl phosphate internal standard. Multiplicities of NMR resonances are reported as s = singlet, d = doublet, t = triplet, m = multiplet, and br = broad. For the NMR chemical shift data of host–guest complexes, *host* denotes signals corresponding to assembly **1** and *encaps* denotes signals corresponding to the encapsulated guest; only encapsulated guest signals are tabulated. All mass spectra were recorded at the UC Berkeley Mass Spectrometry facility. Mass spectra of all host–guest assemblies were acquired on a Waters QTOF API mass spectrometer from methanol, and all other mass spectra were acquired on a Thermo Scientific LTQ-Orbitrap XL mass spectrometer.

2,4,6-Trimethylbenzyl Trimethylphosphonium Chloride (2[Cl]).

To a degassed solution of α²-chloroisodurene (1.0 g, 5.9 mmol) in 20 mL of ether was added trimethylphosphine (1.5 mL, 15 mmol) via syringe, and the solution was stirred for 24 h. The resulting white precipitate was collected by filtration, dissolved in a minimal amount of methylene chloride, and precipitated with excess diethyl ether, and residual solvent was removed overnight under vacuum to give 1.19 g (83%) of a fluffy white solid. ¹H NMR (400 MHz, D₂O): δ 6.90 (s, 2H, ArH), 3.62 (d, *J*_{PH} = 15.4 Hz, 2H, CH₂), 2.16 (s, 6H, *o*-ArCH₃), 2.13 (s, 3H, *p*-ArCH₃), 1.73 (d, *J*_{PH} = 14.2 Hz, 9H, P(CH₃)₃). ¹³C{¹H} NMR (100 MHz, D₂O): δ 138.3 (d, *J*_{CP} = 4.4 Hz, ArC), 137.7 (d, *J*_{CP} = 5.9 Hz, ArC), 129.6 (d, *J*_{CP} = 3.7

Hz, ArC), 122.8 (d, *J*_{CP} = 9.5 Hz, ArC), 24.1 (d, *J*_{CP} = 50.5 Hz, CH₂), 20.0 (s, c), 19.8 (s, d), 8.2 (d, *J*_{CP} = 54.2 Hz, a). ³¹P{¹H} NMR (202 MHz, D₂O): δ 28.2 (s). MS (ESIHR) for C₁₃H₂₂P, calcd (found) *m/z*: 209.1454 (209.1455).

K₁₁[2 ⊂ 1]. The title host–guest complex was prepared *in situ* by mixing 2[Cl] (2.70 mg, 0.011 mmol) and host K₁₁[**1**] (20.0 mg, 0.006 mmol) in 800 μL of CD₃OD (5% DMSO-*d*₆) in an NMR tube. For ¹H NMR (500 MHz, CD₃OD/5% DMSO-*d*₆), due to a very broad aromatic host region at room temperature, only encapsulated guest peaks are tabulated; see Figure S37 for full ¹H NMR spectrum: δ 4.80 (s, 1H, *encaps* ArH), 3.78 (s, 1H, *encaps* ArH), 0.68 (s, 3H, *encaps* ArCH₃), 0.64 (s, 3H, *encaps* ArCH₃), 0.54 (s, 3H, *encaps* ArCH₃), 0.18 (m, 2H, *encaps* CH₂), –0.75 (d, *J*_{PH} = 13.4 Hz, 9H, *encaps* P(CH₃)₃). ³¹P{¹H} NMR (243 MHz, CD₃OD/5% DMSO-*d*₆): δ 26.2 (s, *encaps* 2). HRMS (ESI-QTOF): calcd (found) *m/z*: [**1** + **2** + 8K⁺]^{3–} 1119.6914 (1119.6898), [**1** + **2** + H⁺ + 7K⁺]^{3–} 1107.0394 (1107.0388), [**1** + **2** 2H⁺ + 6K⁺]^{3–} 1094.3876 (1094.3870), [**1** + **2** + 7K⁺]^{4–} 830.0278 (830.0230), [**1** + **2** + H⁺ + 6K⁺]^{4–} 820.5389 (820.5378), [**1** + **2** + 2H⁺ + 5K⁺]^{4–} 810.7999 (810.7924), [**1** + **2** + H⁺ + 5K⁺]^{5–} 648.4385 (648.4313), [**1** + **2** + 2H⁺ + 4K⁺]^{5–} 641.0474 (641.0477).

2,6-Dimethylbenzyl Trimethylphosphonium Chloride (3[Cl]).

The title compound was prepared analogously to compound **2** from 2,6-dimethylbenzyl chloride (400 mg, 2.6 mmol) and trimethyl phosphine (0.53 mL, 5.2 mmol). The product was isolated as a white solid with yield: 104 mg (17%). ¹H NMR (500 MHz, D₂O): δ 7.18 (br, m, 3H, ArH), 3.79 (d, *J*_{PH} = 16 Hz, 2H, benzyl CH₂), 2.32 (s, 6H, ArCH₃), 1.85 (d, *J*_{PH} = 14.1 Hz, 9H, PMe₃). ¹³C{¹H} NMR (125 MHz, D₂O): δ 137.7 (d, *J*_{PC} = 5.8 Hz, ArC), 128.9 (d, *J*_{PC} = 3.6 Hz, ArC), 128.1 (d, *J*_{PC} = 4.1 Hz, ArC), 126.0 (d, *J*_{PC} = 8.6 Hz, ArC), 24.3 (d, *J*_{PC} = 50.4 Hz, benzyl CH₂), 20.1 (s, ArCH₃), 8.2 (d, *J*_{PC} = 54 Hz, PMe₃). ³¹P{¹H} NMR (202 MHz, D₂O): δ 27.1 (s). MS (ESIHR) for C₁₂H₂₀P, calcd (found) *m/z*: 195.1297 (195.1296).

K₁₁[3 ⊂ 1]. The title host–guest complex was prepared *in situ* by mixing 3[Cl] (2.56 mg, 0.011 mmol) and host K₁₁[**1**] (20.0 mg, 0.006 mmol) in 800 μL of CD₃OD (5% DMSO-*d*₆) in an NMR tube. ¹H NMR (500 MHz, CD₃OD/5% DMSO-*d*₆): δ 13.49 (s, *host* NH), 8.05 (br, 12H, *host* ArH), 7.66 (d, *J*_{HH} = 8.70 Hz, 12H, *host* ArH), 7.34 (d, *J*_{HH} = 8.1 Hz, 12H, *host* ArH), 6.97 (t, *J*_{HH} = 8.1 Hz, 12H, *host* ArH), 6.74 (d, *J*_{HH} = 7.6 Hz, 12H, *host* ArH), 6.60 (t, *J*_{HH} = 8.1 Hz, 12H, *host* ArH), 4.88 (t of d, ²*J*_{HH} = 7.5 Hz, ³*J*_{HH} = 2.6 Hz, 1H, *encaps* ArH), 4.54 (br, 1H, *encaps* ArH), 4.19 (br, 1H, *encaps* ArH), 0.17 (s, 6H, *encaps* ArCH₃), –0.02 (m, *J*_{PH} = 14.6 Hz, 2H *encaps* benzyl CH₂), –1.12 (d, *J* = 13.5 Hz, 9H, *encaps* PMe₃). ³¹P{¹H} NMR (243 MHz, CD₃OD/5% DMSO-*d*₆): δ 25.8 (s, *encaps* 3). (ESI-QTOF): calcd (found) *m/z*: [**1** + **3** + 8K⁺]^{3–} 1115.0195 (1115.0140), [**1** + **3** + H⁺ + 7K⁺]^{3–} 1102.3676 (1102.3652), [**1** + **3** + 2H⁺ + 6K⁺]^{3–} 1089.7157 (1089.7036), [**1** + **3** + 7K⁺]^{4–} 826.5239 (826.5271), [**1** + **3** + H⁺ + 6K⁺]^{4–} 817.0349 (817.0303), [**1** + **3** + 2H⁺ + 5K⁺]^{4–} 807.5460 (807.5465), [**1** + **3** + H⁺ + 5K⁺]^{5–} 645.8353 (645.8375), [**1** + **3** + 2H⁺ + 4K⁺]^{5–} 638.0442 (638.0410).

2,4,6-Trimethylbenzyl Triethylphosphonium Chloride (4[Cl]).

The title compound was prepared analogously to compound 2[Cl] starting with α²-chloroisodurene (300 mg, 1.8 mmol) and triethylphosphine (0.8 mL, 5.3 mmol), which gave 125 mg (30%) of a white solid after workup. ¹H NMR (500 MHz, D₂O): δ 6.87 (s, 2H, ArH), 3.52 (d, *J*_{PH} = 14.5 Hz, 2H, CH₂), 2.16 (s, 6H, *ortho*-ArCH₃), 2.09 (s, 3H, *para*-ArCH₃), 2.08 (m, 6H, PCH₂CH₃), 0.99 (d of t, *J*_{PH} = 18.0 Hz, *J*_{HH} = 7.6 Hz, 9H, PCH₂CH₃). ¹³C{¹H} NMR (100 MHz, D₂O): δ 138.3 (d, *J*_{PC} = 3.8 Hz, ArC), 137.5 (d, *J*_{PC} = 4.7 Hz, ArC), 129.5 (d, *J*_{PC} = 3.1 Hz, ArC), 122.9 (d, *J*_{PC} = 8.5 Hz, ArC), 20.1 (s, ArCH₃), 19.8 (d, *J*_{PC} = 46.2 Hz, CH₂), 19.7 (s, ArCH₃), 12.4 (d, *J*_{PC} = 47.8 Hz, PCH₂CH₃), 4.6 (s, PCH₂CH₃). ³¹P{¹H} NMR (202 MHz, D₂O): δ 38.0 (s). MS (ESIHR) for C₁₆H₂₈P, calcd (found) *m/z*: 251.1923 (251.1924).

K₁₁[4 ⊂ 1]. The title host–guest complex was prepared *in situ* by mixing 4[Cl] (3.19 mg, 0.011 mmol) and host K₁₁[**1**] (20.0 mg,

(63) Alaimo, P. J.; Peters, D. W.; Arnold, J.; Bergman, R. G. *J. Chem. Educ.* **2001**, *78*, 64.

0.006 mmol) in 800 μL of CD_3OD (5% $\text{DMSO-}d_6$) in an NMR tube. For ^1H NMR (500 MHz, $\text{CD}_3\text{OD}/5\%$ $\text{DMSO-}d_6$), due to a very broad aromatic host region at room temperature, only encapsulated guest peaks are tabulated; see Figure S38 for full ^1H NMR spectrum: δ 4.98 (s, 1H, *encaps* ArH), 4.22 (s, 1H, *encaps* ArH), 1.42 (s, 3H, *encaps* ArCH_3), 1.08 (s, 3H, *encaps* ArCH_3), 0.63 (s, 3H, *encaps* ArCH_3), 0.44 (m, 2H, *encaps* CH_2), -0.90 (m, 9H, *encaps* PCH_2CH_3), -1.10 (m, 6H, *encaps* PCH_2CH_3). $^{31}\text{P}\{^1\text{H}\}$ NMR (243 MHz, $\text{CD}_3\text{OD}/5\%$ $\text{DMSO-}d_6$): δ 36.1 (s, *encaps* **4**). HRMS (ESI-QTOF): calcd (found) m/z : [**1** + **4** + 8K^+] $^{3-}$ 1133.7070 (1133.6980), [**1** + **4** + H^+ + 7K^+] $^{3-}$ 1121.0552 (1121.0425), [**1** + **4** + 2H^+ + 6K^+] $^{3-}$ 1108.4032 (1108.3844), [**1** + **4** + 6K^+ + H^+] $^{4-}$ 830.8006 (830.7920), [**1** + **4** + 5K^+ + 2H^+] $^{4-}$ 821.5617 (821.5452), [**1** + **4** + 2H^+ + 4K^+] $^{5-}$ 649.4568 (649.4437).

2,6-Dimethylbenzyl- d_2 Alcohol. A 250 mL Schlenk flask was charged with a stir bar, and lithium aluminum deuteride (2.54 g, 60.6 mmol), purged with nitrogen, and diethyl ether (60 mL) were added *via* cannula to form a gray slurry. An addition funnel was added to the Schlenk flask and charged with 2,6-dimethylbenzoic acid (1.3 g, 8.7 mmol) dissolved in diethyl ether (30 mL). The acid solution was slowly added dropwise over 45 min to the LAD solution with vigorous stirring. Once the addition was complete, the addition funnel was replaced with a reflux condenser and the heterogeneous reaction mixture was heated at reflux for 5 days. The resulting suspension was cooled to 0 $^\circ\text{C}$, and a saturated aqueous solution of sodium sulfate was slowly added dropwise until any unreacted LAD had been quenched. Significant heat was evolved as the LAD was quenched, and care was taken to add the aqueous solution slowly enough that the reaction mixture stayed cool during quenching. The precipitated inorganic solids were removed by vacuum filtration over a bed of Celite and washed with diethyl ether (3×50 mL) and water (50 mL). The layers of the filtrate were separated, the aqueous layer was washed with diethyl ether (2×30 mL), and the organics were combined and dried over sodium sulfate. The sodium sulfate was removed by vacuum filtration, and the diethyl ether was removed under reduced pressure to yield an off-white solid (857 mg, 71%). ^1H NMR (600 MHz, CDCl_3): δ 7.14 (t, $J_{\text{HH}} = 7.4$ Hz, 1H, ArH), 7.06 (d, $J_{\text{HH}} = 7.5$ Hz, 2H, ArH), 3.47 (s, 1H, OH), 2.43 (s, 6H, ArCH_3). $^2\text{H}\{^1\text{H}\}$ NMR (92 MHz, CDCl_3): δ 4.59 (s, CD_2). $^{13}\text{C}\{^1\text{H}\}$ NMR (151 MHz, CDCl_3): δ 137.4, 136.4, 128.2, 127.8 (s, ArC), 57.9 (quintet, $J_{\text{CD}} = 21.6$ Hz, CD_2), 19.2 (s, ArCH_3).

2,6-Dimethylbenzyl- d_2 Bromide. A 250 mL round-bottom flask was charged with a stir bar and 2,6-dimethylbenzyl- d_2 alcohol (850 mg, 6.15 mmol) dissolved in diethyl ether (100 mL). The solution was sparged with nitrogen and cooled to -50 $^\circ\text{C}$ with a dry ice/isopropyl alcohol cold bath. Phosphorus tribromide (0.71 mL, 7.40 mmol) was added dropwise to the reaction solution over 15 min by syringe. The solution was allowed to slowly warm to room temperature and stirred overnight (16 h) under nitrogen, during which time the solution changed from colorless to faint orange. The reaction was quenched by pouring the solution over ice (50 mL). The layers were separated, and the aqueous layer was washed with diethyl ether (2×50 mL). The organic layers were combined, washed with a saturated aqueous solution of sodium bicarbonate (75 mL), and dried with magnesium sulfate. The magnesium sulfate was removed by vacuum filtration, and the diethyl ether was removed under reduced pressure to yield a white solid (600 mg, 49%). ^1H NMR (500 MHz, CDCl_3): δ 7.09 (t, $J_{\text{HH}} = 7.5$ Hz, 1H, ArH), 7.02 (d, $J_{\text{HH}} = 7.5$ Hz, 2H, ArH), 2.40 (s, 6H, ArCH_3). $^2\text{H}\{^1\text{H}\}$ NMR (77 MHz, CDCl_3): δ 4.56 (s, CD_2). $^{13}\text{C}\{^1\text{H}\}$ NMR (151 MHz, CDCl_3): δ 137.7, 134.1, 129.5, 128.8 (s, ArC), 19.6 (s, ArCH_3).

2,6-Dimethylbenzyl- d_2 Triethylphosphonium Bromide (5[Br]**).** The title compound was prepared analogously to **2[Cl]** starting from 2,6-dimethylbenzyl- d_2 bromide (550 mg, 2.73 mmol) and triethylphosphine (0.81 mL, 5.47 mmol). After workup, 754 mg of white solid (87%) were obtained. ^1H NMR (600 MHz, D_2O): δ 7.17 (br, 3H, ArH), 2.33 (s, 6H, ArCH_3), 2.23 (br m, 6H, PCH_2CH_3), 1.13

(br m, 9H, PCH_2CH_3). ^2H NMR (92 MHz, D_2O): δ 3.65 (br, CD_2). $^{13}\text{C}\{^1\text{H}\}$ NMR (151 MHz, D_2O): δ 137.6 (d, $J = 4.2$ Hz, ArC), 129.0 (d, $J = 2.8$ Hz, ArC), 128.2 (d, $J = 3.3$ Hz, ArC), 126.2 (d, $J = 8.3$ Hz, ArC), 20.3 (s, ArCH_3), 12.6 (d, $J = 48$ Hz, PCH_2CH_3), 4.8 (d, $J = 5.6$ Hz, PCH_2CH_3). $^{31}\text{P}\{^1\text{H}\}$ NMR (243 MHz, D_2O): δ 37.9 (s). (ESIHR) for $\text{C}_{15}\text{H}_{24}\text{D}_2\text{P}$, calcd (found) m/z : 239.1890 (239.1892).

K₁₁[5** \subset **1**].** The title host–guest complex was prepared *in situ* by mixing **5[Br]** (3.05 mg, 0.011 mmol) and host **1** (20.0 mg, 0.006 mmol) in 800 μL of CD_3OD (5% $\text{DMSO-}d_6$) in an NMR tube. ^1H NMR (500 MHz, $\text{CD}_3\text{OD}/5\%$ $\text{DMSO-}d_6$): δ 8.26 (br, 12H, *host* ArH), 7.75 (br, 12H, *host* ArH), 7.31 (d, $J_{\text{HH}} = 8.3$ Hz, 12H, *host* ArH), 6.63 (d, $J_{\text{HH}} = 7.3$ Hz, 12H, *host* ArH), 6.39 (t, $J_{\text{HH}} = 7.8$ Hz, 12H, *host* ArH), 5.30 (t of d, $^3J_{\text{HH}} = 7.7$ Hz, $^4J_{\text{HH}} = 2.3$ Hz, 1H, *encaps* ArH), 5.04 (d, $J_{\text{HH}} = 7.6$ Hz, 1H, *encaps* ArH), 0.98 (s, 3H, *encaps* ArCH_3), 0.38 (s, 3H, *encaps* ArCH_3), -0.79 (d of t, $J_{\text{PH}} = 18.3$ Hz, $J_{\text{HH}} = 7.6$ Hz, 9H, *encaps* PCH_2CH_3), -1.18 (m, 6H, PCH_2CH_3). $^{31}\text{P}\{^1\text{H}\}$ NMR (243 MHz, $\text{CD}_3\text{OD}/5\%$ $\text{DMSO-}d_6$): δ 35.8 (s, *encaps* **5**). HRMS (ESI-QTOF): calcd (found) m/z : [**1** + **5** + 8K^+] $^{3-}$ 1129.7061 (1129.7013), [**1** + **5** + H^+ + 7K^+] $^{3-}$ 1117.0541 (1117.0553), [**1** + **5** + 2H^+ + 6K^+] $^{3-}$ 1104.4022 (1104.3950), [**1** + **5** + 7K^+] $^{4-}$ 837.5388 (837.5270), [**1** + **5** + H^+ + 6K^+] $^{4-}$ 828.0498 (828.0517), [**1** + **5** + 2H^+ + 5K^+] $^{4-}$ 818.5609 (818.5566), [**1** + **5** + H^+ + 5K^+] $^{5-}$ 654.4473 (654.4441), [**1** + **5** + 2H^+ + 4K^+] $^{5-}$ 646.8561 (646.8483).

2,3,4,5,6-Pentamethylbenzyl Trimethylphosphonium Bromide (6[Br]**).** The title compound was prepared analogously to compound **2[Cl]** starting from 2,3,4,5,6-pentamethyl benzyl bromide (325 mg, 1.30 mmol) and trimethyl phosphine (0.42 mL, 4.00 mmol). The product was isolated as a white solid with a yield of 330 mg (77%). ^1H NMR (500 MHz, D_2O): δ 3.90 (d, $J_{\text{PH}} = 15.5$ Hz, 2H, benzyl CH_2), 2.22 (m, 15H, ArCH_3), 1.79 (d, $J_{\text{PH}} = 14.1$ Hz, 9H, PMe_3). $^{13}\text{C}\{^1\text{H}\}$ NMR (125 MHz, D_2O): δ 135.5 (d, $J = 4.4$ Hz, ArC), 134.4 (d, $J = 3.6$ Hz, ArC), 133.1 (d, $J = 5.4$ Hz, ArC), 122.8 (d, $J = 9.0$ Hz, ArC), 24.8 (d, $J_{\text{CP}} = 50.5$ Hz, CH_2), 17.7 (d, $J = 1.6$ Hz, ArCH_3), 16.1 (s, ArCH_3), 16.0 (d, $J = 1.2$ Hz, ArCH_3), 7.8 (d, $J_{\text{CP}} = 54.1$ Hz, PMe_3). $^{31}\text{P}\{^1\text{H}\}$ NMR (162 MHz, D_2O): δ 28.3 (s). (ESIHR) for $\text{C}_{15}\text{H}_{26}\text{P}$, calcd (found) m/z : 237.1767 (237.1767).

K₁₁[6** \subset **1**].** The title host–guest complex was prepared *in situ* by mixing guest **6** (3.52 mg, 0.011 mmol) and host **1** (20.0 mg, 0.006 mmol) in 800 μL of CD_3OD (5% $\text{DMSO-}d_6$) in an NMR tube. ^1H NMR (500 MHz, $\text{CD}_3\text{OD}/5\%$ $\text{DMSO-}d_6$): δ 8.02 (br, 12H, *host* ArH), 7.66 (br, 12H, *host* ArH), 7.19 (d, $J_{\text{HH}} = 8.5$ Hz, 12H, *host* ArH), 6.95 (br, 12H, *host* ArH), 6.57 (d, $J_{\text{HH}} = 7.7$ Hz, *host* 12H, ArH), 6.28 (t, $J_{\text{HH}} = 8.1$ Hz, 12H, *host* ArH), 0.96 (s, 3H, *encaps* ArCH_3), 0.16 (s, 3H, *encaps* CH_3), -0.09 (s, 3H, *encaps* CH_3), -0.13 (s, 3H, *encaps* CH_3), -0.22 (s, 3H, *encaps* CH_3), -0.47 (d, $J_{\text{PH}} = 13.0$ Hz, 9H, *encaps* PMe_3). HRMS (ESI-QTOF): calcd (found) m/z : [**1** $^{12-}$ + 6^+ + 8K^+] $^{3-}$ 1129.0352 (1129.0127), [**1** $^{12-}$ + 6^+ + H^+ + 7K^+] $^{3-}$ 1116.3833 (1116.3582), [**1** $^{12-}$ + 6^+ + 2H^+ + 6K^+] $^{3-}$ 1103.1313 (1103.7015), [**1** $^{12-}$ + 6^+ + 7K^+] $^{4-}$ 837.0356 (837.0129), [**1** $^{12-}$ + 6^+ + H^+ + 6K^+] $^{4-}$ 827.2967 (827.2755), [**1** $^{12-}$ + 6^+ + 2H^+ + 5K^+] $^{4-}$ 817.8077 (817.7846), [**1** $^{12-}$ + 6^+ + 6K^+] $^{5-}$ 661.8359 (661.8124), [**1** $^{12-}$ + 6^+ + H^+ + 5K^+] $^{5-}$ 654.2448 (654.2300).

2,4,6-Trimethyl-3-chloromethylbenzyl Trimethylphosphonium Chloride (7[Cl]**).** 2,4-Bis(chloromethyl)-1,3,5-trimethylbenzene (500 mg, 2.3 mmol) was dissolved in 130 mL of diethyl ether in a 250 mL Schlenk flask with a stir bar. The solution was sparged with nitrogen for 15 min, and trimethyl phosphine (0.24 mL, 2.3 mmol) was added *via* syringe. The solution was stirred under a nitrogen atmosphere for 2 days after which time the resulting white solid was collected by vacuum filtration and washed with diethyl ether (2×50 mL) and the residual solvent was removed overnight under vacuum. Yield = 70 mg (10%). ^1H NMR (400 MHz, CD_3OD): δ 7.05 (s, 1H, ArH), 4.75 (s, 2H, CH_2Cl), 3.90 (d, $J_{\text{PH}} = 12.8$ Hz, 2H, CH_2P), 2.44 (s, 3H, ArCH_3), 2.38 (s, 3H, ArCH_3), 2.34 (s, 3H, ArCH_3), 1.86 (d, $J_{\text{PH}} = 11.6$ Hz, 9H, PMe_3). $^{13}\text{C}\{^1\text{H}\}$ NMR (125 MHz, CH_3OD): δ 137.9 (d, $J = 5.4$ Hz, ArC), 137.5 (d, $J = 4.3$

Hz, ArC), 136.9 (d, $J = 5.4$ Hz, ArC), 133.8 (d, $J = 3.7$ Hz, ArC), 131.1 (d, $J = 3.7$ Hz, ArC), 124.1 (d, $J = 9.3$ Hz, ArC), 40.9 (s, CH₂Cl), 24.3 (d, $J_{CP} = 49.8$ Hz, CH₂P), 20.1 (d, $J_{CP} = 1.7$ Hz, ArCH₃), 17.8 (d, $J_{CP} = 1.3$ Hz, ArCH₃), 15.7 (d, $J_{CP} = 1.7$ Hz, ArCH₃), 7.4 (d, $J_{CP} = 54.2$ Hz, PMe₃). ³¹P{¹H} NMR (162 MHz, CH₃OD): δ 28.3 (s). (ESIHR) for C₁₄H₂₃ClP, calcd (found) m/z : 257.1220 (257.1223).

2,4,6-Trimethyl-3-chloromethylbenzyl Triethylphosphonium Chloride (8[Cl]). The title compound was prepared from 2,4-bis(chloromethyl)-1,3,5-trimethylbenzene (500 mg, 2.3 mmol) and triethyl phosphine (0.31 mL, 2.1 mmol) analogously to compound 7[Cl]. Yield = 36 mg (5%). ¹H NMR (600 MHz, CH₃OD): δ 7.06 (s, 1H, ArH), 4.76 (s, 2H, CH₂Cl), 3.86 (d, $J_{PH} = 14.6$ Hz, CH₂P), 2.46 (br, 3H, ArCH₃), 2.39 (br, 6H, 2 \times ArCH₃), 2.29 (m, 6H, PCH₂CH₃), 1.16 (d of t, 9H, $J_{PH} = 18.1$ Hz, $J_{HH} = 7.6$ Hz, PCH₂CH₃). ¹³C{¹H} NMR (151 MHz, CH₃OD): δ 138.1 (m, 2 \times ArC), 137.2 (d, $J = 7.6$ Hz, ArC), 134.3 (d, $J = 3.2$ Hz, ArC), 131.5 (d, $J = 3.2$ Hz, ArC), 124.7 (d, $J = 8.9$ Hz, ArC), 41.2 (s, CH₂Cl), 21.0 (d, $J_{CP} = 0.8$ Hz, ArCH₃), 18.3 (d, $J_{CP} = 0.8$ Hz, ArCH₃), 16.2 (d, $J_{CP} = 1.2$ Hz, ArCH₃), 12.8 (d, $J_{CP} = 47.8$ Hz, PCH₂CH₃), 4.7 (d, $J_{CP} = 5.6$ Hz, PCH₂CH₃). ³¹P{¹H} NMR (243 MHz, CH₃OD): δ 38.5 (s). (ESIHR) for C₁₇H₂₉ClP, calcd (found) m/z : 299.1690 (299.1692).

Solid-State Structure of K₇2₄[2 C 1]. X-ray quality single crystals of the host–guest complex [2 C 1]¹¹⁻ were grown by diffusing acetone into a DMF/MeOH solution of host 1 and guest 2 at 5 °C. Diffraction data were collected on a Bruker MicroStar-H X8 APEXII diffractometer with a Bruker APEXII-CCD area detector using Cu K α radiation. Data were integrated using SAINT,⁶⁴ and an absorption correction was applied using SADABS⁶⁵ (within the Apex2 software suite). The structure was solved using direct methods (SIR92) and refined using Fourier techniques in SHELX-97.⁶⁶ Table 3 lists some of the crystallographic data and structural refinement information. Further refinement details and a discussion of the disorder modeling can be found in the Supporting Information.

(64) SAINT: SAX Area-Detector Integration Program; Siemens Industrial Automation, Inc.: Madison, WI, 1999.

(65) Sheldrick, G. M. SADABS: Siemens Area Detector Absorption Correction Program; University of Gottingen: Germany, 2005.

(66) Sheldrick, G. M. SHELX97: Programs for Crystal Structure Analysis; Institut für Anorganische Chemie der Universität: Gottingen, Germany, 1998.

Table 3. Crystallographic Data and Structural Refinement Information for the Solid-State Structure of Host–Guest Complex K₇2₄[2 C 1]

Formula	C _{214.5} H _{216.5} Ga ₄ K ₃ N ₁₃ O _{44.25} P ₅
Molecular weight	4235.54
Crystal appearance, color	Plate, yellow
Crystal dimensions (max, med, min/mm)	0.12 \times 0.8 \times 0.1
Crystal system	Triclinic
Space group	<i>P</i> $\bar{1}$
<i>a</i> (Å)	20.380(4)
<i>b</i> (Å)	20.556(4)
<i>c</i> (Å)	35.192(7)
α (deg)	90.28(3)
β (deg)	92.80(3)
γ (deg)	109.91(3)
Volume (Å ³), <i>Z</i>	13841(5), 2
Absorption coefficient, μ (mm ⁻¹)	1.611
Reflections collected/unique	99023/33712
Goodness-of-fit on F^2	1.097
Final R indices [$I > 2\sigma(I)$]	R1 = 0.1038, wR2 = 0.3028

Acknowledgment. The authors would like to thank Dr. Jamin Krinsky and Dr. Kathleen Durkin for assistance with computational and modeling studies and acknowledge NSF Grants CHE-0233882 and CHE-0840505, which fund the UC Berkeley Molecular Graphics and Computational Facility. We also thank Dr. Michael Pluth, Dr. Carmelo Sgarlata, Courtney Hastings, and Casey Brown for helpful discussions. This work has been supported by the Director, Office of Science, Office of Basic Energy Sciences, and the Division of Chemical Sciences, Geosciences, and Biosciences of the U.S. Department of Energy at LBNL under Contract No. DE-AC02-05CH11231 and an NSF predoctoral fellowship to J.S.M.

Supporting Information Available: SIR fits and measured rate constants for guest bond rotation and exchange, Eyring plots used to determine activation parameters for bond rotation, additional NMR spectra of host–guest complexes, and refinement details for the solid-state host–guest structure. This material is available free of charge via the Internet at <http://pubs.acs.org>.

JA107656G